

## Mppt and Simulation for a Grid-Connected Photovoltaic System and Fault Analysis

<sup>1</sup>K.Manohar, <sup>2</sup>P.Sobha Rani

<sup>1</sup>Scholar M.Tech, Department of Electrical and Electronics Engineering, NBKRIST, AP, India,

<sup>2</sup>Associate Professor, Department of Electrical and Electronics Engineering, NBKRIST, AP, India.

### Abstract

This paper establishes a dynamic model of grid-connected PV system by Matlab/Simulink with d-and q-axis as coordinates which is synchronously rotating with the grid voltage to reflect the characteristics of the system accurately. Based on the accurate modeling system, maximum power point tracking (MPPT) and fault analysis are studied. Grid-connected PV system includes a PV array, a control system, a distribution network and a load. The control system of grid-connected PV system has two effective control strategies. First one is the current control strategy can regulate the current at the point of common coupling to achieve power factor control and regulate the dc link voltage. Second one is the voltage control strategy is used for PV output voltage to achieve closed-loop control which can smoothly and quickly track the maximum power point of PV array. Maximum power point tracking (MPPT) can effectively improve the solar energy conversion efficiency of PV systems. In this paper, Perturb-and-observe (P&O) method is used to achieve this function. Finally fault analysis is carried by creating a LLLG fault in the distribution network and observes the ac voltage, ac current and ac power waveforms at the grid with and without a LLLG fault.

**Keywords** - grid-connected photovoltaic (PV) system, maximum power point tracking, voltage source inverter, and LLLG fault etc...

Date Of Submission:1, December, 2012

Date Of Publication: 15, December 2012

### 1. Introduction

Solar energy has become a very potential new energy. Grid-connected photovoltaic (PV) system does not require bulk and lossy battery and reduces transmission losses. As Conventional sources of energy are rapidly depleting and the cost of energy is rising, photovoltaic energy becomes a promising alternative source. Among its advantages are that it is: 1) abundant; 2) pollution free; 3) distributed throughout the earth; and 4) clean and noise-free source of electricity. The main drawbacks are that the initial installation cost is considerably high and the energy conversion efficiency is relatively low. To overcome these problems, the following two essential ways can be used: 1) increase the efficiency of conversion for the solar array and 2) maximize the output power from the solar array. In recent years, PV system has become one of the main ways to use solar energy. To understand and analyze the performance of a grid connected PV system, simulation software of a grid connected PV system is required. Grid –connected photovoltaic system is shown in fig.1.It includes a PV array, a voltage source inverter (VSI), a control system, a distribution network, a load and a grid. The PV array consists of a number of individual photovoltaic cells that are connected in series and parallel array to convert sunlight to electricity by the use of the photovoltaic effect. The PV array produces the dc power, and hence power electronics and control equipment points are required to convert dc to ac power. A voltage source inverter (VSI) is used to convert dc

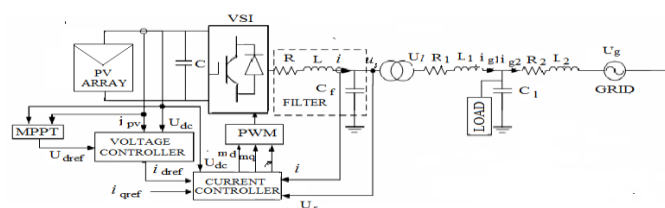


Fig 1: Grid-connected photovoltaic system

power produced by PV array into ac power and this ac power is injected into the utility grid. The control system consists of current control strategy and voltage control strategy. Current control strategy is used to achieve the dc voltage regulation at dc link and unity power factor at grid and the voltage control strategy is applied to achieve maximum power point tracking. Maximum power point tracking (MPPT) can effectively improve the solar energy conversion efficiency of PV systems. In this paper, Perturb-and-observe (P&O) method is used to achieve this function. This paper establishes a Dynamic model of grid-connected PV system by Matlab/Simulink with d- and q-axis as coordinates which is synchronously rotating with the grid voltage to reflect the characteristics of the system accurately. Based on the accurate modeling system, analyze the performance of PV systems for different irradiances, maximum power point tracking and finally fault analysis is carried by creating a LLLG fault in the distribution network and observe the ac voltage , ac current and ac power waveforms at the grid with and without a LLLG fault.

## 2. Dynamic Model Of Grid-Connected PHOTOVOLTAIC SYSTEM

A typical single-stage grid-connected PV system is shown in Fig.1. A PV array is connected to a distribution network with a voltage source converter (VSC). In order to analysis and control conveniently, dq components in d- and q-axis are presented.

### 2.1. Photovoltaic System Model

As reported in literature [6], PV arrays consist of series connected cells which are actually diodes, thus the equivalent circuit is represented by a current source parallel to an ideal diode. The mathematical modeling of PV arrays is given:

$$i_{pv} = n_p I_{ph} - n_p I_{rs} \left[ \exp \frac{q u_{dc}}{A k T} \left( u_{dc} + \frac{n_s R_s i_{pv}}{n_p} \right) - 1 \right] - I_{rsh} \quad \text{--- (1)}$$

Where  $u_{dc}$  is PV arrays voltage,  $n_p$  and  $n_s$  are the number of PV cells connected in parallel and in series respectively,  $I_{ph}$  is the photocurrent of a single solar module which is proportional to both illumination and surface area,  $I_{rs}$  is the saturation current of diode which is related to temperature,  $k$  is Boltzman constant (1.38e-23, in Joules per Kelvin),  $q$  is electric charge (1.6e-19, in Coulombs),  $T$  is operating temperature,  $A$  is P-N junction ideal factor.  $R_s$  is series resistance of the single solar module, and  $I_{rsh}$  is the current flowing through the shunt resistance. Ignoring the power absorbed by the inductance and the resistance of the VSC interface [9], the dynamic equations of the PV system are:

$$C \frac{du_{dc}}{dt} = i_{pv} - \frac{m_d}{2} i_d - \frac{m_q}{2} i_q \quad \text{--- (1.1)}$$

$$L \frac{di_q}{dt} = -R i_q + L \omega i_d + \frac{u_{dc}}{2} m_q - v_{sq} \quad \text{--- (1.2)}$$

$$L \frac{di_d}{dt} = -R i_d - L \omega i_q + \frac{u_{dc}}{2} m_d - v_{sd} \quad \text{--- (1.3)}$$

Where  $C$  is dc-link capacitance,  $i_d$  and  $i_q$  are the d- and q-axis currents on the converter side,  $u_{sd}$  and  $u_{sq}$  are d- and q-axis components of VSC filtered voltage,  $L$  and  $R$  are resistance and inductance of the,  $m_d$  and  $m_q$  are control signal of VSC.

### 2.2. Distribution Network Model

According to Fig. 1, we can get the reference model of the distribution network as follows:

$$\frac{di_{g1d}}{dt} = -\frac{R_1}{L_1} i_{g1d} + \omega i_{g1q} + \frac{N}{L_1} u_{sd} - \frac{1}{L_1} u_{1d} \quad \text{--- (2.1)}$$

$$\frac{di_{g1q}}{dt} = -\frac{R_1}{L_1} i_{g1q} - \omega i_{g1d} + \frac{N}{L_1} u_{sq} - \frac{1}{L_1} u_{1q} \quad \text{--- (2.2)}$$

$$\frac{di_{g2d}}{dt} = -\frac{R_2}{L_2} i_{g2d} + \omega i_{g2q} + \frac{N}{L_2} u_{sd} - \frac{1}{L_2} u_{1d} \quad \text{--- (2.3)}$$

$$\frac{di_{g2q}}{dt} = -\frac{R_2}{L_2}i_{g2q} - \omega i_{g2d} + \frac{N}{L_2}u_{sq} - \frac{1}{L_2}u_{1q} \quad (2.4)$$

$$\frac{du_{sd}}{dt} = \omega u_{sq} + \frac{1}{c_f}i_d - \frac{N}{c_f}i_{g1d} \quad (2.5)$$

$$\frac{du_{sq}}{dt} = -\omega u_{sd} + \frac{1}{c_f}i_q - \frac{N}{c_f}i_{g1q} \quad (2.6)$$

$$\frac{du_{1d}}{dt} = -\frac{1}{c_1}i_{g1d} - \frac{1}{c_1}i_{g2d} + \omega u_{1q} - u_{1d} \quad (2.7)$$

$$\frac{du_{1q}}{dt} = \frac{1}{c_1}i_{g1q} - \frac{1}{c_1}i_{g2q} - \omega u_{1d} - u_{1q} \quad (2.8)$$

Where  $i_{g1d}$  and  $i_{g1q}$  are d- and q-axis components of the current between the VSC interface and the load,  $i_{g2d}$  and  $i_{g2q}$  are d- and q-axis components of the current between the load and the grid,  $R_1$  and  $L_1$  are resistance and inductance between the VSC interface and the load,  $R_2$  and  $L_2$  are resistance and inductance between the load and the grid,  $u_{1d}$  and  $u_{1q}$  are d and q-axis components of load voltage,  $N$  is the transformer turns ratio,  $C_f$  is filter capacitance,  $C_1$  is power-factor correction capacitance, and  $\omega$  is the dq-system angular speed.

### 2.3. Load Model

The load model considered in this paper is a series R-L circuit, it is shown as follows:

$$\frac{di_{1d}}{dt} = \omega i_{1q} - \frac{R_1}{L_1}i_{1d} + \frac{1}{L_1}u_{1d} \quad (2.9)$$

$$\frac{di_{1q}}{dt} = -\omega i_{1d} - \frac{R_1}{L_1}i_{1q} + \frac{1}{L_1}u_{1q} \quad (2.10)$$

Where  $R_1$  and  $L_1$  are resistance and inductance of the load,  $i_{1d}$  and  $i_{1q}$  are d- and q-axis components of the load current.

## 3. Pv System Control

### 3.1. Current Control

In order to control the grid current, power, frequency and power factor efficiently, it is necessary to transform the three-phase ac signals into proper dq-frame counterparts. Thus, the controllers process dc equivalents rather than original sinusoidally-varying signals[8]. The block diagram of dq-frame current control is shown in Fig. 2. The control inputs  $m_d$  and  $m_q$  are given as [5]:

$$m_d = \frac{2}{U_{dc}} [U_d - L\omega i_q + U_{sd}] \quad (3.1)$$

$$m_q = \frac{2}{U_{dc}} [U_q - L\omega i_d + U_{sq}] \quad (3.2)$$

By controlling the values  $m_d$  and  $m_q$  in equations (3.1) & (3.2),  $i_d$  and  $i_q$  rapidly track their respective reference commands  $i_{dref}$  and  $i_{qref}$ . And then active and reactive outputs of PV system are expressed as [5]:

$$P_s = \frac{3}{2} U_{sd} i_d \quad (3.3)$$

$$Q_s = -\frac{3}{2} U_{sd} i_q \quad (3.4)$$

From the above equations (3.3) & (3.4),  $P_s$  and  $Q_s$  are controlled by controlling the  $i_d$  and  $i_q$ . Control of the q-axis current at 0 (i.e  $i_q=0$  then  $Q_s = 0$  and power factor =  $\frac{\text{active power}(P_s)}{\text{apparent power}(P_s+Q_s)} = \text{unity}$ .) will enable power factor unity.

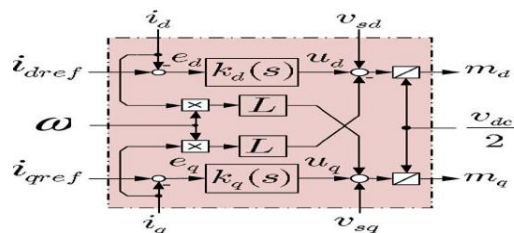


Fig 2: dq-frame current control scheme

### 3.2 Voltage Control

The purpose of voltage control is to make dc-link voltage track the voltage which corresponds to the maximum power point. The dc-link voltage is given as

$$u_{dc} = \frac{1}{c} \int i_c dt \quad \text{--- (3.5)}$$

where  $c$  = capacitance of dc-link and  $i_c$  = dc-link current but

$$i_c = i_{pv} - i_d \quad \text{--- (3.6)}$$

$$u_{dc} = \frac{1}{c} \int (i_{pv} - i_d) dt \quad \text{--- (3.7)}$$

taking laplace transform on both sides

$$u_{dc}(s) = \frac{1}{cs} [i_{pv}(s) - i_d(s)] \quad \text{--- (3.8)}$$

from[5],

$$i_d(s) = G_i(s) i_{dref}(s) = \frac{1}{Ts+1} i_{dref}(s) \quad \text{--- (3.9)}$$

Normally, the time constant  $T$  takes as 0.5ms.

$$i_{dref}(s) = G_u(s) [u_{dref}(s) - u_{dc}(s)] \quad \text{--- (3.10)}$$

where  $G_u(s)$  is a proportional-integral compensator =  $K_p + \frac{K_i}{s}$

Where,  $K_p$  and  $K_i$  are the proportion coefficient and integral coefficient, respectively.

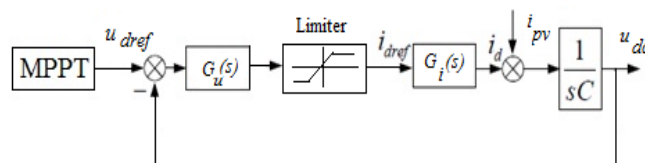
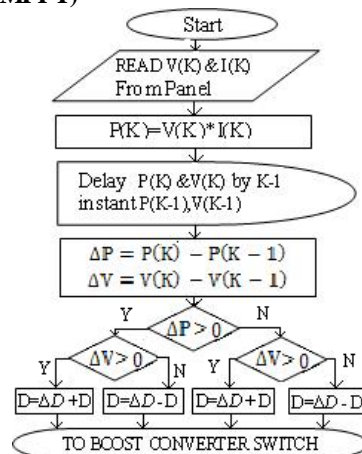


Fig 3: DC-link voltage control scheme

Fig.3 shows block diagram of dc-link control scheme. MPPT track  $u_{dref}(s)$  corresponding to maximum power.  $u_{dc}(s)$  compare with  $u_{dref}(s)$  then error signal is given to a proportional-integral compensator. This proportional-integral compensator set the  $i_{dref}(s)$ . This  $i_{dref}(s)$  processed through current controller and set the  $i_d(s)$ . The  $i_{pv}(s) - i_d(s)$  processed through an integrator and set  $u_{dc}$  corresponding to  $u_{dref}(s)$ . In this way dc-link voltage is controlled. The limiter protect PV system against external faults.

### 3.3 Maximum Power Point Tracking (MPPT)



D=Duty cycle &  $\Delta D$  =Perturbation

Fig 4: Flow Chart for MPPT Algorithm

MPPT can effectively improve the solar energy conversion efficiency of PV systems. In this paper, Perturb-and-observe (P&O) method is used to achieve this function [7]. P&O method first measures the voltage  $V(K)$  and current  $I(K)$  then determine power  $P(K) = V(K) * I(K)$ . This current output power of the array  $P(K)$  compare with

P(K-1), and then adds a small perturbation ( $\Delta D$ ) to the original output voltage, after that, compares the current power with the original one. If the power increased, the original disturbance would be used, if the power decreased, the original disturbance should be changed. The control is shown in Fig. 4. MPPT track  $u_{dref}$  corresponding to maximum power.

#### 4. Matlab-Based Simulation and Results

##### 4.1 Simulation of PV System

In fig.6, PV array consists of six PV modules connected in series altogether generating 133V dc voltage. Basically PV module can be implemented as voltage input type PV module or Current input type PV module. In this paper Current input type PV module is implemented in simulink. The simulink model for single PV module is shown in fig.5. PV module parameters are shown in tabular column 2.

|                     |   |
|---------------------|---|
| Inputs to PV module | <ul style="list-style-type: none"> <li>• PV current <math>I_{pv}</math> [A]</li> <li>• Insolation [W/m<sup>2</sup>]</li> </ul>            |
| Outputs             | <ul style="list-style-type: none"> <li>• PV voltage <math>V_{pv}</math> [V]</li> <li>• PV output power <math>P_{pv}</math> [W]</li> </ul> |

**Table 1:** Tabular column for current input PV module

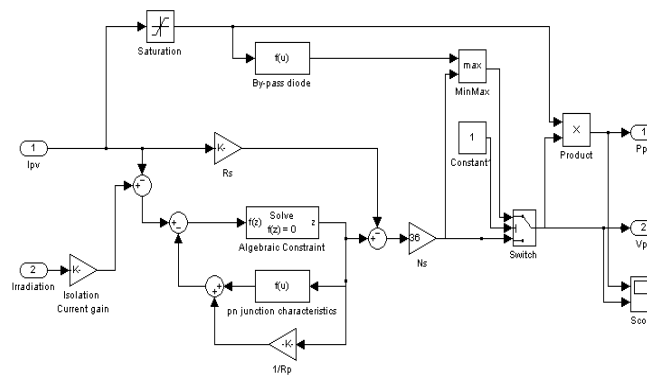


**Fig 5:** Single PV Module Simulink Model

|   |           |
|---|-----------|
| open-circuit voltage $V_{oc}$ (volts)                   | 22.2      |
| short-circuit current $I_{sc}$ (amps)                   | 5.45      |
| rated current $I_R$ at maximum power point (MPP) (amps) | 17.2      |
| rated voltage $V_R$ at MPP (volts)                      | 4.92      |
| pn-junction reverses saturation current ( $I_o$ )(amps) | 2.615e-01 |
| Irradiation to short circuit current gain (G)           | 0.00545   |
| Cell Parallel Resistance ( $R_p$ ) ( $\Omega$ )         | 2.742     |
| Cell Series Resistance ( $R_s$ ) ( $\Omega$ )           | 0.01309   |
| Default no. of cells in Series ( $N_s$ )                | 36        |

**Table 2:** Tabular column for PV module parameters

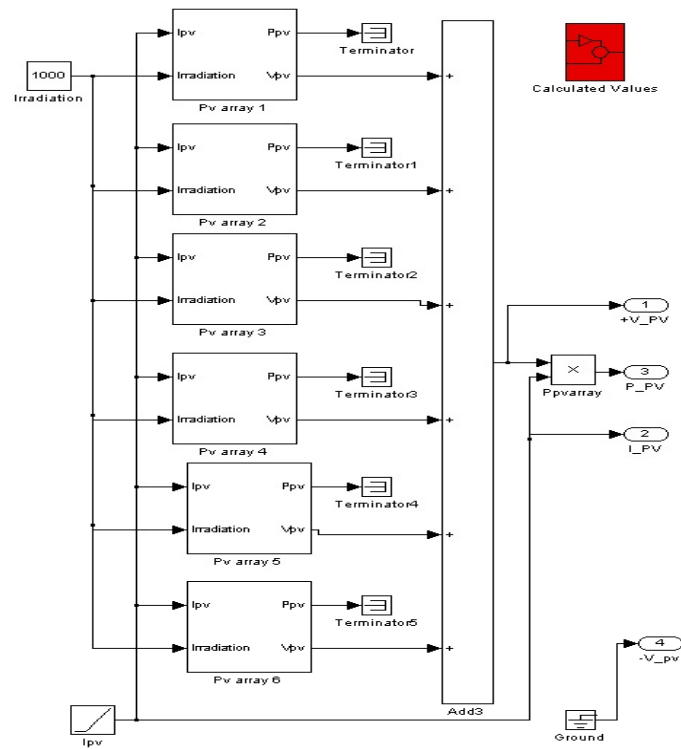


Fig 6: PV array simulink model

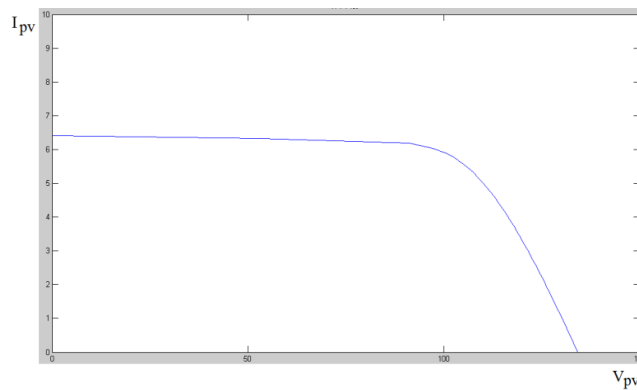


Fig 7: I-V Characteristics of PV array

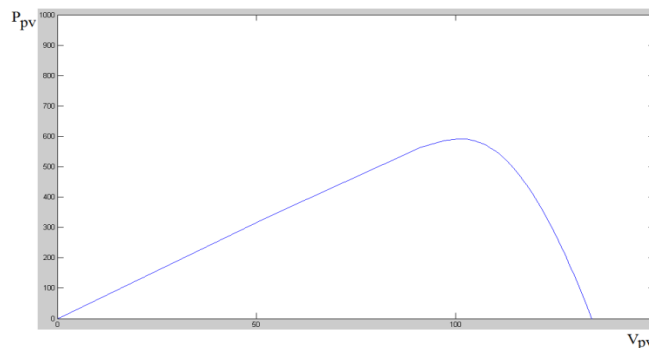
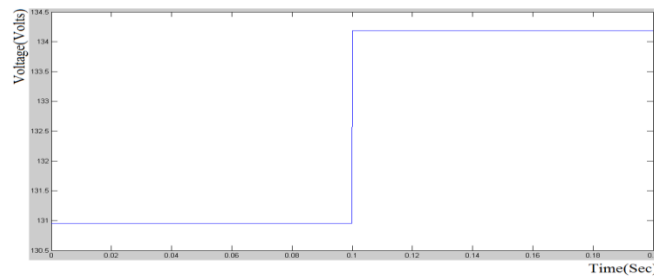


Fig 8: P-V Characteristics of PV array

The I-V Characteristics and P-V Characteristics of PV array when the solar irradiation level is  $1000\text{ W / m}^2$  are shown in fig.7 and fig.8 respectively. PV array generated voltage changes when solar irradiation level changes. Fig.9 shows PV array generated voltage change when solar irradiation level changes from  $500\text{ W/m}^2$  to  $1000\text{ W/m}^2$ .



**Fig 9:** change in array voltage due to sudden increase in Irradiation

#### 4.2 Simulation of Grid-Connected PV system and Fault Analysis

The simulation of grid-connected PV system contain various simulation blocks of PV array, voltage source inverter, filter circuit, distribution network, load, utility grid, current controller, voltage controller, MPPT and phase locked-loop(PLL). In this paper, PV array generates a voltage of 133V dc for a solar irradiance of  $1000\text{W}/\text{m}^2$ , it is observed from fig.10. This dc voltage is converted into ac voltage by a voltage source inverter; it is controlled by space vector pulse width modulation. This ac voltage is step up to 622V(max) i.e. 440V(rms) by a step up transformer as shown in fig.11(a) finally this ac voltage is injected into utility grid. The voltage, current and power wave forms at grid without a fault in the distribution network are shown in fig.11, fig.12 and fig.14 respectively.

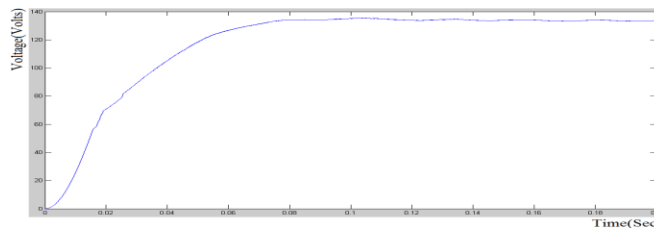


**Fig 10:** Voltage waveform on DC side of VSC

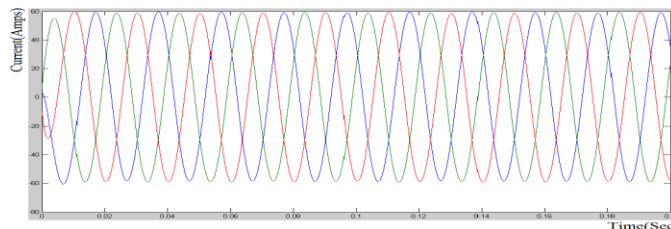


**Fig 11:** Voltage waveform at grid without fault

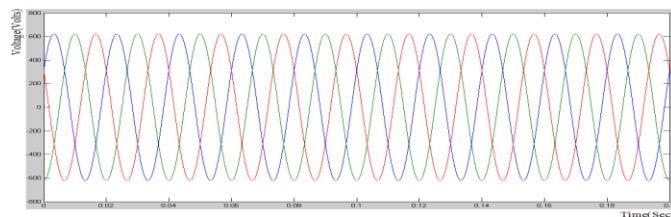


**Fig 12:** Current waveforms at grid without fault

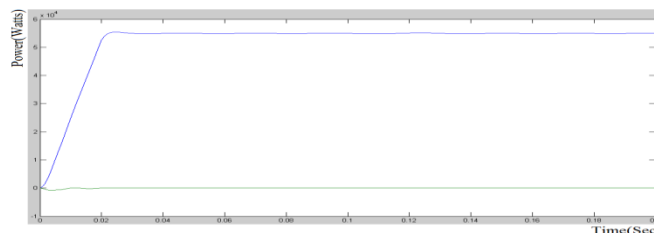


**Fig 14:** Output power at grid supplied by PV systems without a fault

**4.2.1 Fault Analysis**

A three phase to ground (symmetrical) fault is created on the grid side for the purpose of fault analysis on the grid connected PV system, generally three phase faults are most severe faults on the power system. Simulation diagram of grid-connected PV system with a LLLG fault is shown in fig.13. Here a LLLG fault is occur in the distribution network connected between VSI and grid as shown in fig.13. The voltage and current waveforms at grid during the fault are shown in fig.15(a) & 15(b) respectively. The voltage waveform does not alter do to the fault because the grid maintained at constant voltage. The Current before initialize the fault (<.06sec) is maintained at 60A(max) , when a fault is initialized at 0.06 sec the current raises to 225A(max) and finally the current settles to its normal value of 60A(max) after the fault period(80msec).

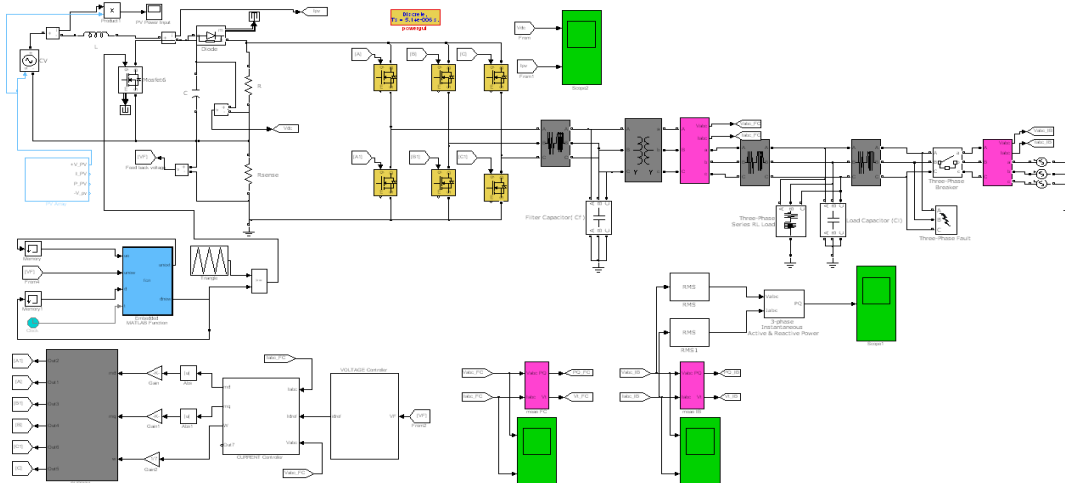


**Fig 13:** simulation diagram of grid-connected PV system with a LLLG fault

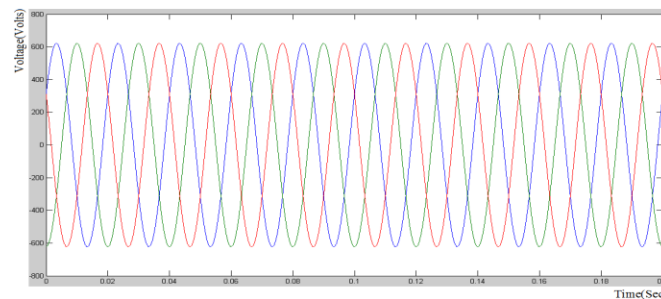


**Fig 15(a):** Three phase voltages on Grid side for a three phase fault

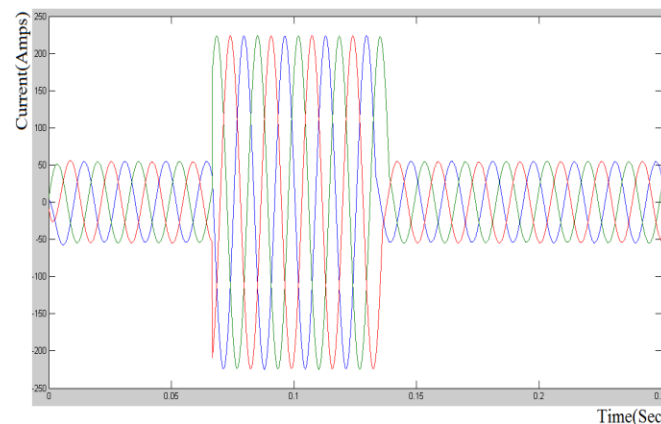


**Fig 15(b):** Three phase currents on Grid side for a three phase fault

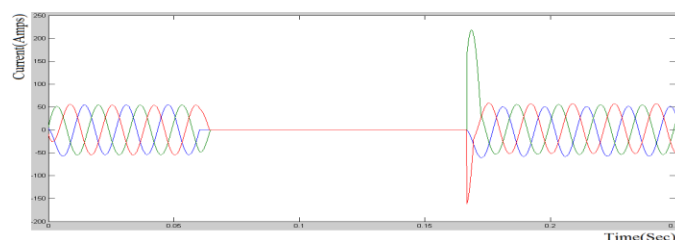


**Fig 16:** Three phase currents on Grid side with circuit breaker

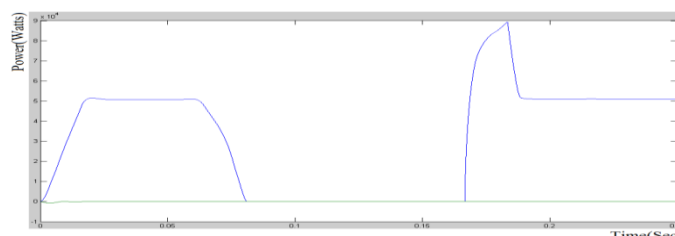


**Fig 17:** Output power at grid supplied by PV systems with circuit breaker

The PV system supplies power to the grid under normal operating conditions and injects high currents during fault which cannot be sustained by the grid. The circuit breaker placed before the grid enables the PV system to incorporate under safe mode only and take care of itself under contingent situations (in this case LLLG fault). The operation of the circuit breaker results in the following current and power variations shown in Fig. 16 & Fig. 17.

## 5. Conclusion

In this paper, a grid-connected PV system based on MATLAB has been proposed. Based on the accurate modeling system, maximum power point tracking (MPPT) and fault analysis are studied. The control consists of a current control strategy and a voltage control strategy. The current control strategy permits dc-link voltage regulation and enables power factor control. Moreover, the current control strategy significantly decouples the dynamics of the PV system from those of the distribution network and loads. Furthermore, it is expected that the current control strategy renders the PV system protected against external faults. The voltage control strategy can achieve the maximum power point tracking and maximization of the real power output of the PV system. The MATLAB/SIMULINK model of a grid-connected photovoltaic (PV) system is useful to understand and master the performance of PV systems and also to optimize the design and lower costs. It is also useful for shortening development cycles as well as improving system reliability and efficiency.

## References:

- [1]. M.Ciobotaru, T.Kerekes, R.Teodorescu, A. Bouscayrol, "PV inverter simulation using MATLAB/Simulink graphical environment and PLECS blockset," IEEE IECON 2006 Annual Conference on Industrial Electronics, pp. 5313-5318, Nov. 2006.
- [2]. S. Oh, M. Sunwoo, "Variable structure PWM controller for high efficient PV inverters," IEEE International Conference on Sustainable Energy Technologies, pp. 24-27, Nov. 2008.
- [3]. A. Bellini, S. Bifaretti, V. Iacovone, "Resonant DC-DC converters for photovoltaic energy generation systems," International Symposium on Power Electronics, Electrical Drives, Automation and Motion, pp. 815-820, Jun. 2008.
- [4]. O.Wasynczuk, N. A. Anwah, "Modeling and dynamic performance of a self-commutated photovoltaic inverter system," IEEE Transaction on Energy Conversion, vol.4, no.3, pp. 322-328, Sep. 1989.
- [5]. A. Yazdani and P.P. Dash, "A Control Methodology and Characterization of Dynamics for a Photovoltaic (PV) System Interfaced with a Distribution Network" IEEE Trans. Power Del., vol. 24, no. 3, pp.1538-1551, Jan. 2009.
- [6]. A.Yazdani and R.Iravani, "An accurate model for the dc-side voltage control of the neutral point diode clamped converter," IEEE Trans.Power Del., vol. 21, no. 1, pp. 185-193, Jan. 2006.
- [7]. Hussein K H, Muta I, Hoshimo T, Oskada M, "Maximum photovoltaic power tracking: an algorithm for rapidly changing atmospheric conditions, generation, transmission and distribution," IEE Proceedings, vol.142, no.1, pp. 59-64, 1995.
- [8]. S.K. Chung, "A phase tracking system for three phase utility interface inverters," IEEE Trans. Power Electron., vol. 15, no. 3, pp. 431-438, May 2000.
- [9]. P.Vas, Vector Control of AC Machines. Oxford, U.K.: Oxford Univ.Press, 1990.